npg

c-Abl and Arg tyrosine kinases regulate lysosomal degradation of the oncoprotein Galectin-3

X Li[1], Q Ma[1], J Wang[2], X Liu[1], Y Yang[1], H Zhao[1], Y Wang[1], Y Jin[1], J Zeng[2], J Li[1], L Song[2], X Li[1], P Li[1], X Qian[2] and C Cao*,[1]

Galectin-3 (Gal3) has important roles in tumor transformation and metastasis. This study shows that c-Abl and Abl-related gene (Arg) associate with and phosphorylate Gal3. The SH (Src homology)3 domains of c-Abl/Arg bind to a P_{80}GPPSGP motif of Gal3, and Tyr79 and Tyr118 are the major tyrosine phosphorylation sites. A consequence of this interaction and phosphorylation is the significant impairment of chaperone-mediated autophagy of Gal3. Cells expressing Gal3 and treated with the c-Abl/Arg inhibitor STI571, Gal3-depleted cells, and Gal3-depleted cells expressing Gal3 phosphorylation mutants all display an increased sensitivity to apoptosis-inducing agents. In addition, tumor cells expressing the phosphorylation mutants show impaired tumorigenicity. These results partially explain the antiapoptotic effect of Abl and Arg. As tumors frequently overexpress Gal3, a c-Abl/Arg-specific inhibitor may potentially be applied along with other antitumor drugs to target the lysosomal degradation of Gal3 in tumor therapy.

Galectin-3 (Gal3) is a 31-kDa galactoside-binding protein with roles in a myriad of cell processes, such as cell growth, adhesion, mitosis, proliferation, angiogenesis, pre-mRNA splicing, and, most importantly, apoptosis.[1] It facilitates neoplastic progression, tumor cell survival, angiogenesis, and tumor metastasis in several human malignancies, including thyroid, gastric, breast, colon, liver, prostate, bladder, brain, and nervous system cancers.[2] Cells overexpressing Gal3 are resistant to a diverse group of apoptotic stimuli by preventing mitochondrial damage, cytochrome *c* release, and caspase activation.[3,4] The antiapoptotic activity of Gal3 is not yet completely understood.[2]

The mammalian Abl nonreceptor tyrosine kinase (c-Abl) and its cytoplasmic homology protein Arg (the Abl-related gene) are modular proteins with multiple functions.[5,6] Both c-Abl and Arg are important for cell proliferation, apoptosis, adhesion, cell migration, and stress responses.[5,6] Mammalian c-Abl and *Caenorhabditis elegans* Abl-1 can function in either the proapoptotic or antiapoptotic pathways in response to DNA damage and other stress signals, depending on the cellular context.[7,8] It is well established that nuclear c-Abl kinase is required for DNA damage-induced apoptosis by interacting with p53 and p73,[9–12] and that kinase active c-Abl is required in reactive oxygen species-induced apoptosis.[13,14] On the other hand, progenitor B cells derived from *c-abl* knockout mice are more sensitive to apoptosis induced by growth factor deprivation and glucocorticoid treatment.[15] Moreover, *abl*$^{-/-}$ *arg*$^{-/-}$ embryos at 10.5–11 dpc exhibit widespread apoptosis in all tissues.[16] Oncogenic forms of abl kinase, including Bcr-Abl, TEV-Abl, Gag-Abl, and ΔSH3 Abl, are strong inhibitors of apoptosis.[17–20] Furthermore, *C. elegans* Abl-1 can antagonize p53-mediated germline

apoptosis after ionizing irradiation.[21] Thus, c-Abl/Arg has both positive and negative roles in apoptosis depending on the cellular context.[22] Several observations suggest that the cytoplasmic localization of c-Abl is required for antiapoptotic function.[23,24] However, the signals that mediate its antiapoptotic effect are largely unknown.

In this paper, we report that Gal3 interacts with and is phosphorylated by the nonreceptor tyrosine kinases c-Abl and Arg, and that the lysosomal-dependent proteolysis of Gal3 is efficiently blocked by the kinases.

Results

c-Abl and Arg associate with Gal3. Using a yeast two-hybrid analysis, we previously showed that c-Abl associates with Gal3. To substantiate the interaction between c-Abl and Gal3, anti-Gal3 immunoprecipitates of human MCF-7 cells were analyzed by immunoblotting with anti-c-Abl. Immunoblotting showed that c-Abl was present in the anti-Gal3 immunoprecipitate, but not in the immunoprecipitate using mouse IgG (belonging to the same subclass) (Figure 1a). To confirm the interaction specificity, Gal3 was knocked down by RNAi, and c-Abl was undetectable in anti-Gal3 immunoprecipitates from MCF-7/*gal3* RNAi cell lysates (Figure 1a). In a reciprocal experiment, Gal3 was found in anti-c-Abl, but not in rabbit IgG, immunoprecipitates (Figure 1b). The c-Abl:Gal3 complex was not disrupted in the presence of lactose, which indicated that the Abl:Gal3 interaction was not mediated through glycoproteins with which c-Abl might interact (Figure 1b). To further show that the interaction occurred in the cell, MCF-7 cells were treated
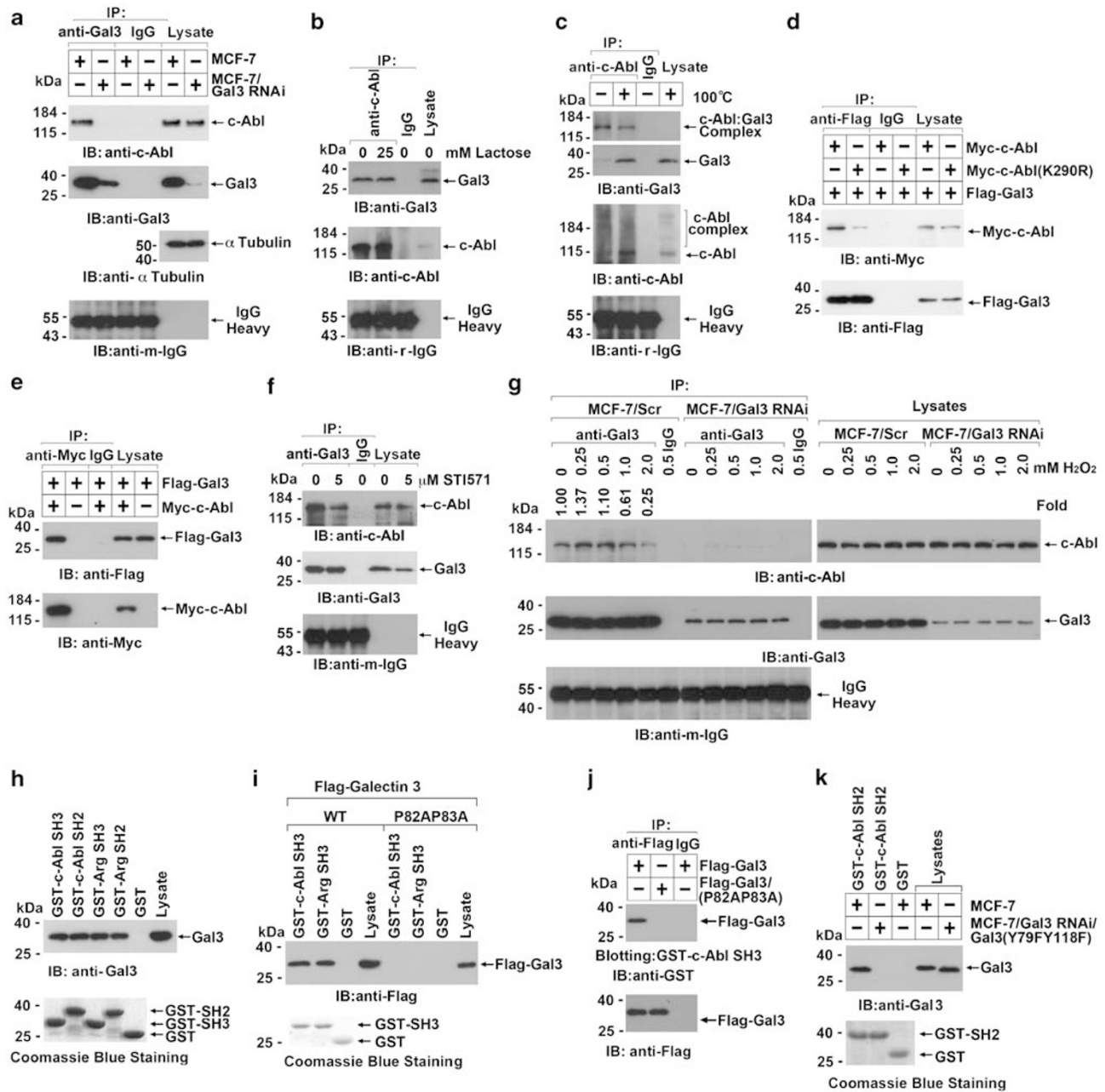
Figure 1 c-Abl and Arg associate with Gal3. (**a**) Lysates from MCF-7 or MCF-7/*gal3* RNAi cells were subjected to immunoprecipitation with anti-Gal3 or normal mouse IgG1 as control, and were subsequently analyzed by immunoblotting with anti-Gal3, anti-c-Abl, or anti-mouse IgG. (**b**) Lysates from MCF-7 cells were subjected to immunoprecipitation with anti-c-Abl in the presence of 0 or 25 mM lactose and analyzed by immunoblotting with anti-Gal3 or anti-c-Abl. (**c**) MCF-7 cells were treated with or without PFA for 30 min and the lysates subjected to immunoprecipitation with anti-c-Abl. The lysates were analyzed by immunoblotting with anti-Gal3 or anti-c-Abl. (**d**, **e**) 293T cells were cotransfected with Flag-Gal3 and Myc-c-Abl or Myc-c-Abl(K290R)-expressing plasmids. The anti-Flag (**d**) or anti-Myc (**e**) immunoprecipitates were analyzed by immunoblotting with anti-Myc or anti-Flag. (**f**) Lysates from MCF-7 cells treated with or without 5 μM STI571 for 8 h were subjected to immunoprecipitation with anti-Gal3. After normalization for the Gal3 level, the adsorbates were subsequently analyzed by immunoblotting with anti-c-Abl or anti-Gal3. (**g**) MCF-7/Scramble or MCF-7/*gal3* RNAi cells were treated with the indicated concentration of H_2O_2. The anti-Gal3 immunoprecipitates were analyzed by immunoblotting with anti-c-Abl and anti-Gal3. (**h**) Lysates from MCF-7 cells or (**i**) 293 cells expressing Flag-Gal3 or Flag-Gal3(P82AP83A) were incubated with the indicated GST fusion protein or GST for 2 h. The adsorbates were analyzed by immunoblotting with anti-Flag. (**j**) Anti-Flag or IgG immunoprecipitates from cells transfected with Flag-Gal3 or Flag-Gal3(P82AP83A) were blotted onto nitrocellulose membrane. The nitrocellulose membrane was incubated with soluble GST-c-Abl SH3 for 2 h and then analyzed with anti-GST or anti-Flag antibody. (**k**) Lysates from MCF-7 and MCF-7/*gal3* RNAi/*gal3*(Y79FY118F)-stable cells were incubated with GST-c-Abl-SH2 or GST agarose beads for 2 h. The adsorbates were analyzed by immunoblotting with anti-Gal3

with the reversible chemical cross-linker PAF. Immuno-blotting of anti-c-Abl immunoprecipitates with anti-Gal3 showed the presence of the Gal3:c-Abl complex, which

was disrupted by incubating at 100°C for 30 min (Figure 1c). In addition, 293T cells were cotransfected with Flag-Gal3 and Myc-c-Abl. Anti-Flag immunoprecipitation showed an
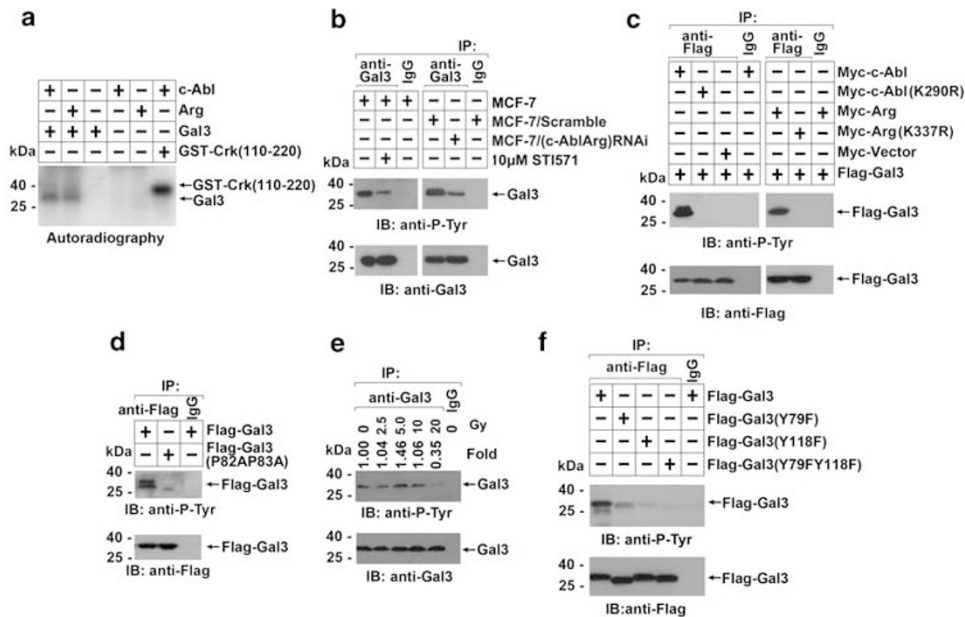
Figure 2 Gal3 was phosphorylated by c-Abl and Arg. (**a**) Recombinant Gal3 (0.5 μg) or GST-Crk(110–220) was incubated with 10 ng of human Abl or Arg protein (Upstate Biotechnology Inc.) in the presence of [γ-^{32}P] ATP. The reaction products were analyzed by autoradiography. (**b**) MCF-7 cells were treated with or without 10 μM STI571 for 12 h. Anti-Gal3 immunoprecipitates were normalized by the Gal3 level, and then analyzed by immunoblotting with anti-P-Tyr or anti-Gal3 (left). Lysates of PepA-treated MCF-7/Scramble or MCF-7/(c-abl + arg) RNAi cells were immunoprecipitated with anti-Gal3, and the immunoprecipitates were analyzed by immunoblotting with anti-P-Tyr or anti-Gal3 after normalization (right). (**c**) c-abl$^{-/-}$ arg$^{-/-}$ MEF cells were cotransfected with the indicated vectors. Anti-Flag immunoprecipitates were analyzed by immunoblotting with anti-P-Tyr or anti-Flag. (**d**) c-abl$^{-/-}$ arg$^{-/-}$ MEF cells were cotransfected with Myc-c-Abl and Flag-Gal3 or Flag-Gal3(P82AP83A). Anti-Flag and IgG immunoprecipitates were analyzed by anti-P-Tyr or anti-Flag. (**e**) MCF-7 cells were treated with γ-irradiation at the indicated dosage. Anti-Gal3 immunoprecipitates were analyzed by immunoblotting with anti-P-Tyr or anti-Gal3. (**f**) 293T cells were cotransfected with myc-c-Abl and Flag-Gal3 or Flag-Gal3 mutants. Anti-Flag immunoprecipitates were analyzed by immunoblotting with anti-P-Tyr or anti-Flag

associated Myc-c-Abl protein in anti-Myc immunoblotting (Figure 1d). A kinase inactive form of c-Abl (c-Abl(K290R), in which the lysine residue in position 290 was replaced by arginine) was observed to interact with Gal3, but to a significantly lesser extent (Figure 1d). Reciprocally, an immunoblot analysis of anti-Myc immunoprecipitates with anti-Flag showed an association between Myc-c-Abl and Flag-Gal3 (Figure 1e). Moreover, Myc-Gal3 was found in anti-Flag immunoprecipitates prepared from cells expressing Myc-Gal3 and Flag-c-Abl (Supplementary Figure 1a). In concert with these findings, an endogenous c-Abl:Gal3 interaction was partially disrupted by the Abl/Arg inhibitor, STI571 (Figure 1f). The Arg kinase also formed complexes with Gal3 (Supplementary Figure 1b). It is known that c-Abl is activated by a low level of H_2O_2[13] or irradiation,[25] whereas a high concentration of H_2O_2 results in the inactivation of c-Abl.[14] We found that treatment with 0.25 and 0.5 mM H_2O_2 results in the slightly increased formation of c-Abl: Gal3 complexes, whereas higher H_2O_2 ($>$1 mM) yielded decreased associations (Figure 1g). As a control, little, if any, c-Abl was present in anti-Gal3 immunoprecipitates of MCF-7/ gal3 RNAi cells (Figure 1g). Similar findings were obtained when the cells were treated with γ-irradiation (Supplementary Figure 1c). These findings indicate that endogenous c-Abl and Arg constitutively associate with endogenous Gal3, but an increased association is observed with enhanced kinase activity.

To further define the interaction between c-Abl and Gal3, lysates from MCF-7 cells were incubated with glutathione S-transferase (GST) or GST fusion proteins. An immunoblot analysis with anti-Gal3 antibody showed the binding of Gal3 to both the Src homology (SH)3 and SH2 domains of c-Abl and Arg (Figure 1h). Gal3 contains a potential SH3-binding motif (Y$_{79}$PGPPSGP). In contrast to Gal3, the binding of c-Abl SH3 or Arg SH3 was eliminated with Gal3(P82AP83A), in which the proline residues in position numbers 82 and 83 of Gal3 were replaced by a similar amino-acid residue alanine (Figure 1i). To rule out indirect binding mediated by other components in the cell lysate, Flag-Gal3 or Flag-Gal3(P82A-P83A) was subjected to SDS-PAGE. Blotting with soluble GST-c-Abl SH3, followed by anti-GST antibody, showed that c-Abl SH3 binds directly to Gal3 but not to Gal3(P82AP83A) (Figure 1j). An association between c-Abl and Gal3 but not Gal3(P82AP83A) indicates that the motif is important for the interaction (Supplementary Figure 1d). Moreover, the c-Abl SH2 domain could not bind to Gal3(Y79FY118F), a mutant in which tyrosine residues at amino-acid residues 79 and 118 were replaced by a similar unphosphorylatable amino-acid residue phenylalanine (Supplementary Figure 1e). This mutant could not be phosphorylated by c-Abl or Arg. (Figures 1k and 2f). These findings show that c-Abl and Arg bind directly to Gal3 through interactions governed by SH3 domains and the PGPPSGP proline-rich motif of Gal3, as well as SH2 domains and the potentially phosphorylated tyrosine residues of Gal3.

Gal3 was phosphorylated by c-Abl and Arg. The association between Gal3 and c-Abl/Arg suggests that
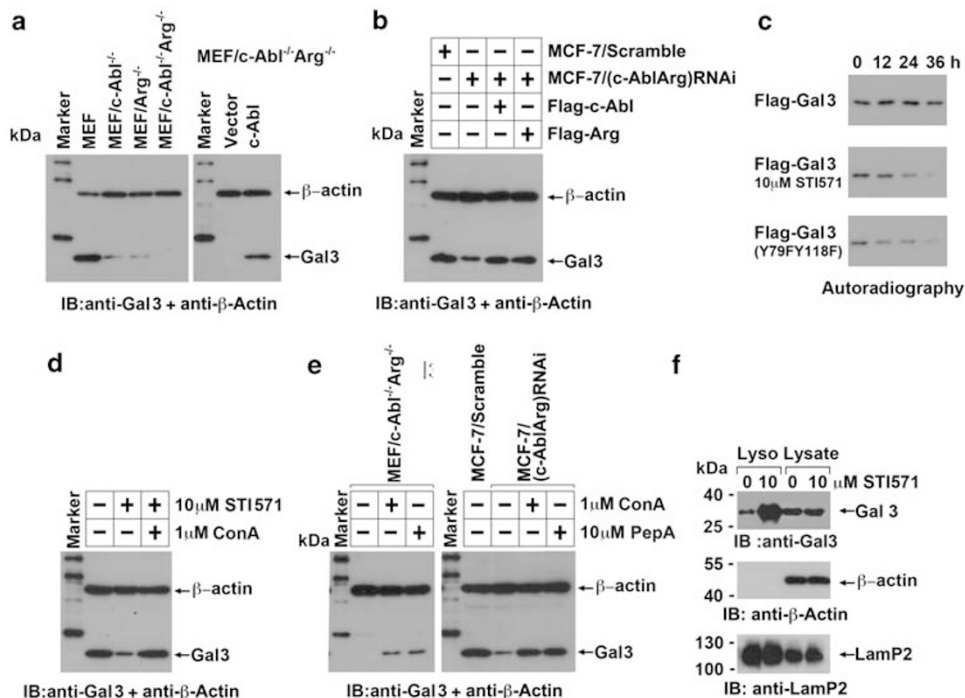
Figure 3 The c-Abl/ Arg phosphorylation inhibits Gal3 autophagy. (**a**, **b**) Lysates from the indicated cells were analyzed by immunoblotting with anti-Gal3 and anti-β-actin. (**c**) 293T cells expressing Flag-Gal3 or Flag-Gal3(Y79FY118F) in the presence of c-Abl were treated with or without 10 μM STI571 for 6 h, followed by a pulsed-chase assay. (**d**) MCF-7 cells were treated with STI571 and/or ConA at the indicated concentration for 16 h. Cell lysates were subjected to immunoblotting with the indicated antibodies. (**e**) c-abl$^{-/-}$ arg$^{-/-}$ MEF cells (left two panels) or MCF-7/(c-abl + arg) RNAi cells (right panel) were treated with or without 1 μM ConA or 10 μM PepA for 16 h. Cell lysates were analyzed by immunoblotting with anti-Gal3 and anti-α tubulin. (**f**) MCF-7 cells were treated with or without 10 μM STI571 for 6 h, and then for another 12 h in the presence of 10 μM PepA. Lysosomes were prepared and analyzed by immunoblotting with the indicated antibodies

Gal3 is a substrate for these tyrosine kinases. To confirm that Gal3 is phosphorylated in vitro, 0.5 μg recombinant Gal3 was incubated with c-Abl or Arg in the presence of [γ-^{32}P]-ATP. An analysis of the reaction products showed the phosphorylation of Gal3 (Figure 2a). Immunoblotting of anti-Gal3 immunoprecipitates from MCF-7 cell lysates with an anti-phosphotyrosine (P-Tyr) antibody showed that Gal3 was constitutively phosphorylated and that the phosphorylation was significantly inhibited by STI571 (Figure 2b, left). Substantially less Gal3 tyrosine phosphorylation was found in MCF-7/(c-abl + arg) RNAi cells compared with MCF-7/Scramble cells (Figure 2b, right; Supplementary Figure 2a). Moreover, Gal3 was phosphorylated by c-Abl and Arg but not by kinase inactive c-Abl(K290R) or Arg(K337R), in which the lysine at the amino-acid residue 290 or 337, respectively, was replaced by similar arginine (Figure 2c). In agreement with the findings that Gal3 binds to c-Abl through the Y79PGPPSGP motif, Gal3(P82AP83A) was not phosphorylated by c-Abl (Figure 2d). Consistent with the findings that the association between c-Abl and Gal3 was regulated by oxidative stress and irradiation, increased phosphorylation was observed when MCF-7 cells were treated with < 10 Gy γ-irradiation (Figure 2e) or 0.25–0.5 mM H_2O_2 (Supplementary Figure 2c), and decreased significantly at higher dosages (Figure 2e and Supplementary Figure 2c).

We next evaluated the c-Abl and Arg phosphorylation sites on Gal3. Flag-Gal3 was cleaved by thrombin at R129 and then

subjected to immunoblotting by anti-P-Tyr. Only the N terminal of Flag-Gal3(1–129), but not Gal3(130–253), was shown to be tyrosine phosphorylated (Supplementary Figure 2d; data not shown). As the N terminal of Gal3 could not be cleaved by any specific proteases for mass spectrometry (MS)/MS analysis, we digested Flag-Gal3 (expressed in the presence of c-Abl) with a less specific elastase and then analyzed the peptides by liquid chromatography (LC)/MS/MS. The results suggested that Y79 was phosphorylated (data not shown). When we further mutated Y79 to a similar amino-acid residue phenylalanine (F), tyrosine phosphorylation decreased, but was not eliminated (Figure 2f), which suggests that there was more than one tyrosine phosphorylation site on Gal3. The tyrosine residues on Gal3 (1–129) were then individually mutated, and the results suggested that the Y118F mutation also resulted in a substantial decrease in tyrosine phosphorylation (Figure 2f and Supplementary Figure 2d). Therefore, the tyrosine phosphorylation of Gal3 primarily occurs on Y79 and is potentially but not actually confirmed by MS/MS on Y118.

c-Abl/Arg-dependent phosphorylation inhibits lysosomal-dependent degradation of Gal3. To confirm that c-Abl and Arg regulate Gal3 levels in cells, cell lysates from wild-type, c-abl$^{-/-}$, arg$^{-/-}$, or c-abl$^{-/-}$ arg$^{-/-}$ mouse embryo fibroblast (MEF) cells were analyzed by immunoblotting with anti-Gal3. Gal3 protein levels were decreased in c-abl$^{-/-}$ and arg$^{-/-}$ MEF cells and, to a

greater extent, in $c\text{-}abl^{-/-}arg^{-/-}$ MEF cells (Figure 3a, left). The exogenous Myc-c-Abl expression in $c\text{-}abl^{-/-}arg^{-/-}$ MEF cells partially restores Gal3 protein levels (Figure 3a, right). Gal3 protein levels were also found to be significantly decreased in MCF-7/(c-abl+arg) RNAi cells, and the expression could be rescued by the overexpression of c-Abl or Arg in which three nucleotides at the 3rd position of amino-acid codon in the RNAi-targeting sequence was mutated (Figure 3b). An analysis of Gal3 in the medium showed that c-Abl/Arg regulates intracellular Gal3 levels by a mechanism other than protein secretion because no more Gal3 was secreted into the medium by MCF-7/(c-abl+arg) RNAi cells (Supplementary Figure 3a). Similarly, when 293 cells were transfected with the same amount of Flag-tagged Gal3 and mutants, the expression levels of Flag-Gal3(Y79FY118F) and Flag-Gal3(P82AP83A), which cannot be phosphorylated by c-Abl/Arg, decreased significantly. Treatment with the c-Abl/Arg inhibitor also resulted in decreased expression of Gal3 (Supplementary Figure 3b). To investigate whether c-Abl and Arg regulate the Gal3 protein half-life, pulse-chase assays were performed using Flag-Gal3 and Flag-Gal3(Y79FY118F)-expressing 293T cells in the presence of 0 or 10 μM STI571, respectively. Flag-Gal3 had a half-life of > 40 h, whereas the half-life was significantly reduced to ~25 h in cells treated with STI571 (Figure 3c). In addition, the half-life of Flag-Gal3(Y79FY118F) was also reduced to ~18 h in the absence of STI571 (Figure 3c). As controls, little if any effect was observed on other abundant proteins in these assays (Supplementary Figure 3c). It is noted that the downregulation of Gal3 levels could be restored by treating cells with the lysosome inhibitor Concanamycin A (ConA) (Figure 3d) or lysosomal protease inhibitor pepstatin A (PepA) (Supplementary Figure 3d), but not with the proteasome inhibitor lactacystin (data not shown). Gal3 expression was also observed to be partially restored when $c\text{-}abl^{-/-}arg^{-/-}$ MEF cells and MCF-7/(c-abl+arg) RNAi cells were treated with ConA or PepA (Figure 3e). In agreement with the findings that a high concentration of H_2O_2 inhibits Gal3 phosphorylation, Gal3 level decreased significantly on treatment with 1 mM H_2O_2 for ≥8 h (data not shown). Furthermore, immediately after STI571 treatment, Gal3 was preferentially bound to lysosomes when compared with other lysosomal degradable proteins, such as IkBα[26] (Figure 3f and Supplementary Figure 3f).

To further show that c-Abl/Arg regulates Gal3 levels by preventing its lysosomal degradation, MCF-7 cells were treated with STI571 or its solvent (DMSO), and stained with anti-Gal3 and anti-Lamp2, a molecular marker of lysosomes. Gal3 was found to be distributed in both the cytoplasm and the nuclear compartments (Figure 4a, upper panel). In contrast, STI571-treated wild-type MCF-7 cells, but not cells expressing STI571-resistant c-Abl, resulted in a decreased level of cellular Gal3, which was found to be accumulated in lysosomes (Figure 4a, second and third rows; Figure 4b, upper panel). Far more Gal3 was accumulated in lysosomes when cells were treated with STI571 in the presence of the lysosomal inhibitor PepA (Figure 4a, fourth and fifth rows; Figure 4b, lower panel). Moreover, the expression of Gal3 was rescued, and the protein was found to be accumulated in

lysosomes by treating MCF-7/(c-abl+arg) RNAi cells with lysosomal inhibitors, whereas Gal3 expression was undetectable by immunostaining in the absence of lysosomal inhibitors (Figure 4a sixth row; Figure 4b, lower panel). However, the unphosphorylated Gal3 mutants expressed in MCF-7/gal3 RNAi cells were also found to aggregate in the lysosomes (Figure 4c, upper two panels; Figure 4d; data not shown). Moreover, wild-type Gal3 was also observed to accumulate in lysosomes when they were stably expressed in MCF-7/(c-abl+arg) RNAi cells (Figure 4c, lower two panels; Figure 4d). Similar results were obtained with other Gal3-expressing tumor cell lines (such as HeLa, H1229, A549, HCT116; data not shown). These data collectively show that, in the absence of kinase active c-Abl and Arg, Gal3 is accumulated in lysosomes and degraded through the lysosomal pathway.

c-Abl and Arg block Gal3 degradation by chaperone-mediated autophagy. Chaperone-mediated autophagy (CMA) is known to occur by transport of the target protein to the lysosomal lumen, mediated by HSC70 and Lamp2.[27] When MCF-7 cells were treated with STI571, Gal3 aggregated with the localization of HSC70 in the lysosome (Figure 5a, left and right panels). However, no Gal3 complexes were observed with LC3, a molecular marker of autophagic vacuoles (AVs) (Figure 5a, lower panel). The lysosomal degradation of Gal3 in the presence of STI571 could be blocked by the lysosomal selective inhibitor ConA, but not by the AV-selective inhibitor 3-methyladenine (3MA) (Figures 3d and e, 5b). Moreover, significantly more HSC70:Gal3 complexes were found by coimmuno-precipitation from the cells treated with STI571 (Figure 5c). In agreement with these findings, Flag-Gal3(P82AP83A) and Flag-Gal3(Y79FY118F) were found to bind to HSC70 to a greater extent than wild-type Gal3 (Figure 5d). These results suggest that Gal3 is degraded through CMA, but not microautophagy or macroautophagy, when it cannot be phosphorylated by c-Abl or Arg.

The c-Abl/Arg-mediated phosphorylation of Gal3 regulates cell apoptosis and tumorigenesis. The effect of tyrosine phosphorylation of Gal3 by c-Abl and Arg on cell apoptosis was assessed. As expected, the depletion of Gal3 by RNAi resulted in significantly more cell apoptosis, as shown by the treatment of cells with 10 Gy IR or 0.5 mM H_2O_2, and the antiapoptotic effect of Gal3 was rescued by the expression of wild-type Gal3 but not Gal3(Y79FY118F) (Figure 6a; data not shown). Similar results were obtained when the cells were treated with other apoptotic stimuli reagents, such as cisplatin or staurosporine (STS). Interestingly, even more apoptotic cells were observed in the context of Gal3(P82AP83A) expression compared with the gal3 knockdown cell line (Figure 6b and data not shown). It was also found that Gal3 degradation induced by the c-Abl/Arg inhibitor STI571 was synergized by apoptotic stimuli, such as STS (Figure 5b). To address this mechanism, we analyzed caspase activation and found that caspase 2 and caspase 6, but not caspase 9 or caspase 12, were activated more by STS treatment in MCF-7/gal3 RNAi cells (Figure 6c). Caspase activation was attenuated by the expression of
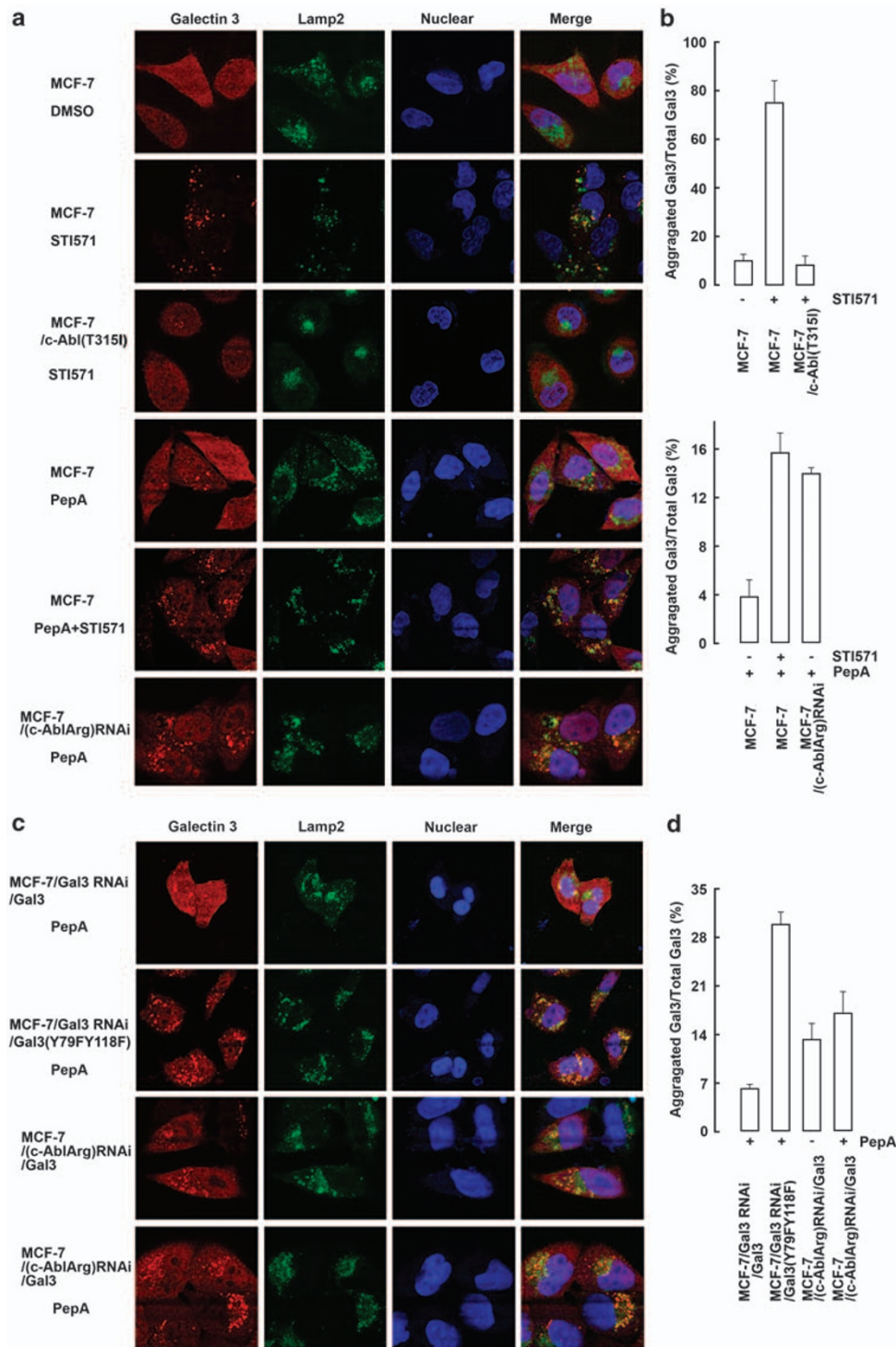
Figure 4 The c-Abl/ Arg phosphorylation inhibits lysosomal accumulation of Gal3. (**a**, **c**) The indicated cell lines were treated with or without STI571 and/or PepA, stained with anti-Gal3, anti-Lamp2 and Hoechst 33342, and then subjected to analysis by laser confocal microscopy. (**b**, **d**) Percentage of Galectin-3 accumulated in lysosomes was assessed

wild-type *Gal3* but not *gal3*(Y79FY118F). Increased mitochondrial cytochrome *c* release, mitochondrial potential loss, and PARP cleavage was also observed in MCF-7/*gal3* RNAi and MCF-7/*gal3* RNAi/Gal3Y79FY118F) cells compared with wild-type MCF-7 and MCF-7/*gal3* RNAi/*gal3*

cells (Figure 6d). These findings are supported by an earlier report that STS induces the apoptosis of MCF-7, a caspase 3-deficient cell line, by the activation of caspase 6.[28] Moreover, Gal3 and Gal3(Y79FY118F) were expressed in c-Abl/Arg-depleted cells (Supplementary Figure 4a). In
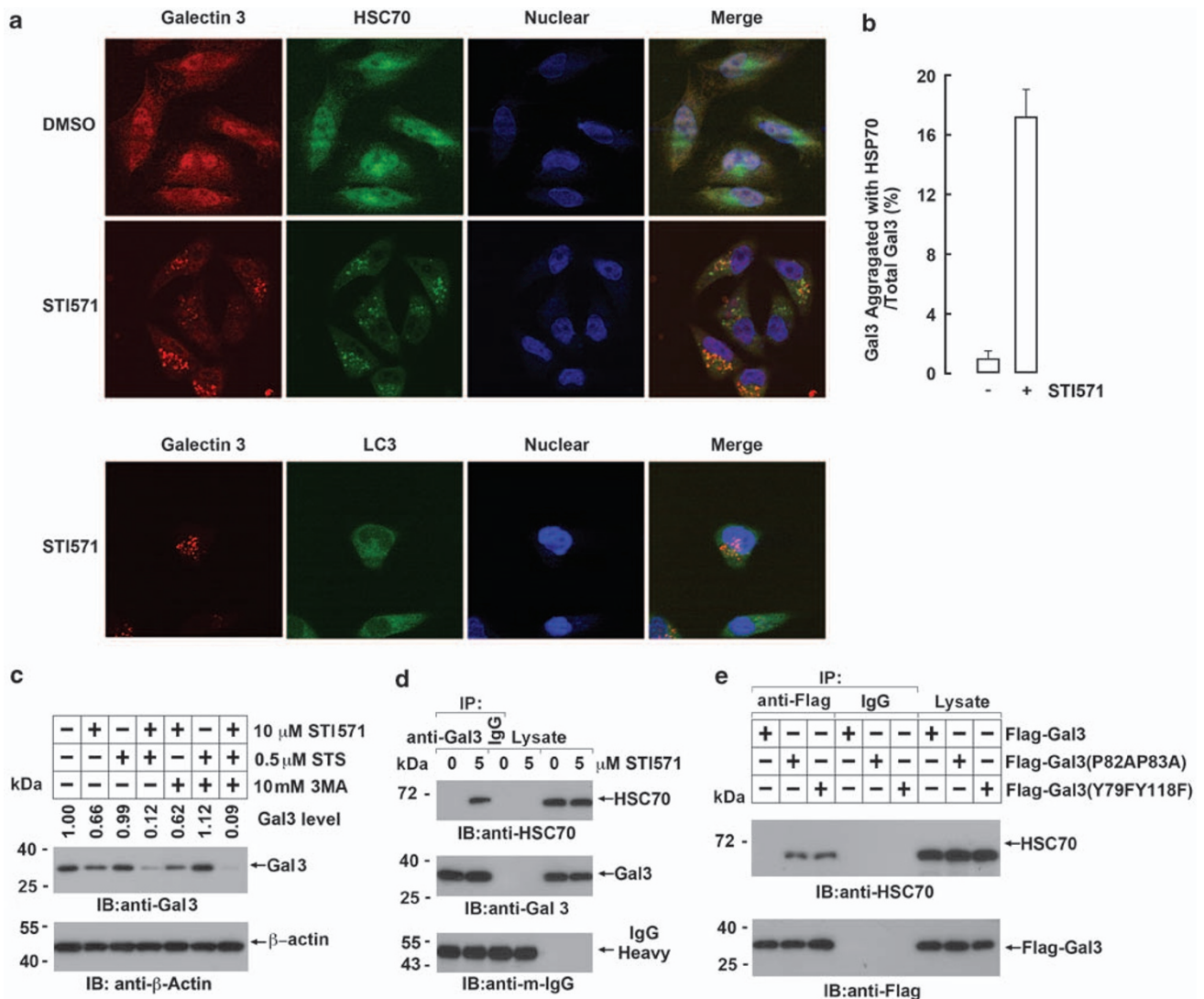
Figure 5 c-Abl/Arg blocks Gal3 degradation by chaperone-mediated autophagy. (**a**) MCF-7 cells were treated with or without 5 μM STI571 for 12 h and stained with anti-Gal3 and anti-HSC70 (upper left panel) or anti-LC3 (lower left panel). The percentage of Galectin-3 accumulated with Hsp70 was accessed (right panel). (**b**) MCF-7 cells were treated with STI571, STS and/or 3MA for 8 h and the cell lysates analyzed by immunoblotting with anti-Gal3 and anti-β-actin. (**c**) Anti-Gal3 immunoprecipitates from MCF-7 cells treated with 0 or 5 μM STI571 were analyzed by immunoblotting with anti-Gal3 and anti-HSC70. (**d**) 293T cells were transfected with 1 μg Flag-Gal3, 4 μg Flag-Gal3(P82AP82A), or 4 μg Flag-Gal3(Y79FY118F). (**e**) Anti-Flag immunoprecipitates were analyzed with anti-HSC70 and anti-Flag

agreement with the findings that $c\text{-}Abl^{-/-}Arg^{-/-}$ MEF cells are more sensitive to apoptotic stimuli,[14,16] MCF-7/($c\text{-}abl + arg$) RNAi cells were sensitized to apoptotic stimuli by STS (Figure 6e). This was slightly attenuated by the overexpression of wild-type Gal3 and to a lesser extent by Gal3(Y79FY118F) (Figure 6e). To further address the c-Abl/Arg-dependent antiapoptotic property of Gal3, a similar investigation was carried out in HeLa cells, and consistent results were obtained (Figure 6f and Supplementary Figure 4b). Caspase 3 and caspase 6 were found to be activated more by STS treatment in HeLa/Gal3 RNAi cells (data not shown). Gal3 expression exhibited little, if any, effect on cell apoptosis in c-Abl/Arg-depleted cells (Figure 6f). These data collectively show that the antiapoptotic activity of Gal3 is dependent on the presence of c-Abl and Arg.

Gal3 is considered to be an oncogenic protein.[29] To investigate whether c-Abl and Arg regulate the tumorigenic effects of Gal3, MCF-7/gal3 RNAi cells and the same cells rescued by the expression of wild-type or non-phosphorylated Gal3 were injected into the flanks of nude mice. Tumor growth was significantly repressed for tumors originating in MCF-7/gal3 RNAi cells. Furthermore, the phenotype was rescued by the expression of wild-type Gal3 but not the non-phosphorylated Gal3 mutants. In agreement with the findings from the in vitro apoptosis assay in Figure 6a, tumors induced by MCF-7/gal3 RNAi cells rescued by the expression of unphosphorylated Gal3(P82AP83A) or Gal3(Y79FY118F) were significantly smaller than the MCF-7/gal3 RNAi cells. No tumors were observed in the three and four mice, respectively, of the seven inoculated mice per group (Figures 7a, c). Consistent with the findings that MCF-7/
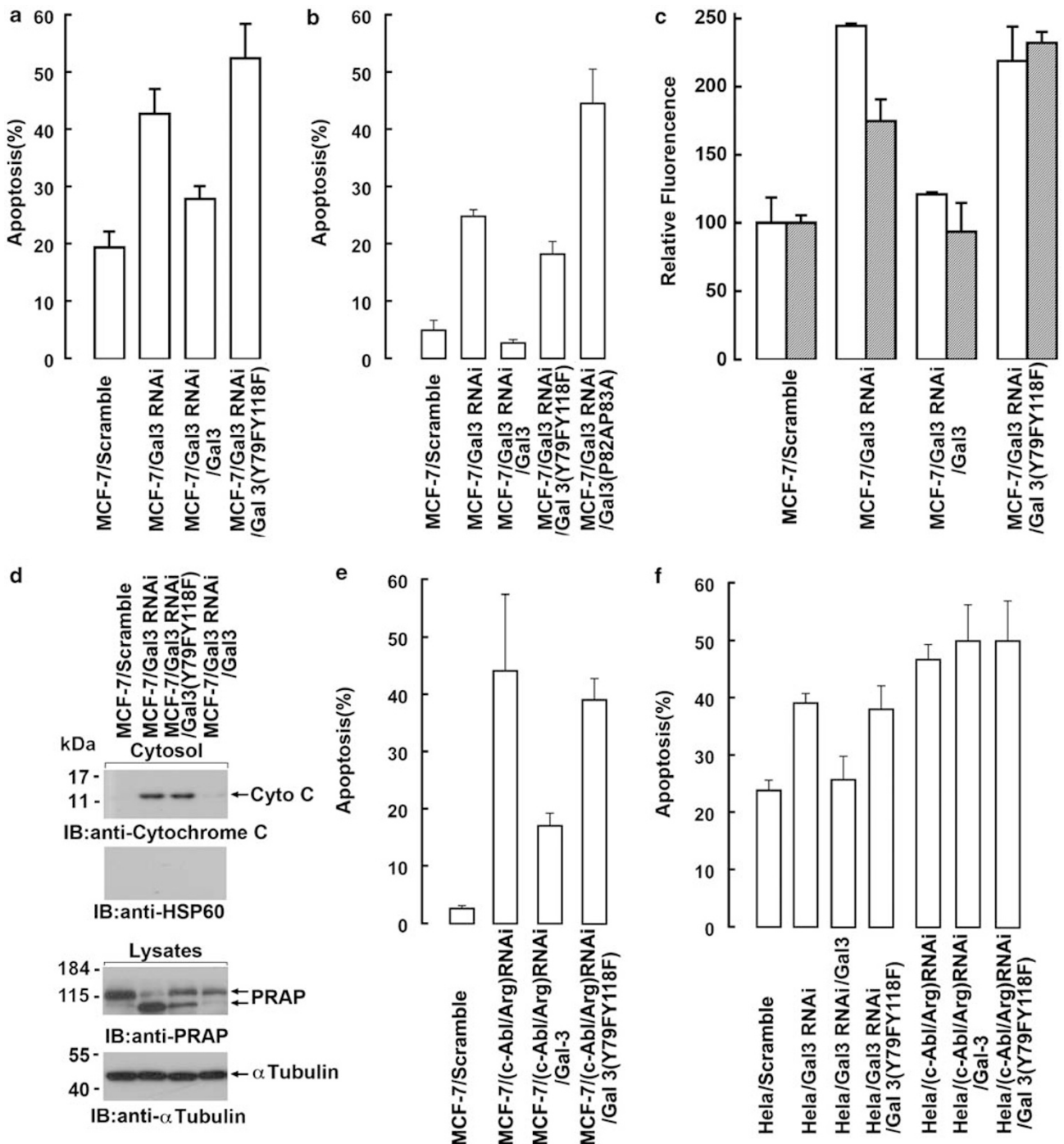
Gal3 is regulated by Abl tyrosine kinases
X Li *et al*
1284

Figure 6 The c-Abl/Arg-mediated phosphorylation of Gal3 regulates cell apoptosis. (**a**) The indicated cells were treated with 10 Gy IR and harvested 48 h after treatment, and cell apoptosis was assessed by Sub-G1. (**b**) The indicated cells were treated with 4 μM CDDP for 24 h. Cell apoptosis was assessed by Sub-G1. (**c**) The indicated cells were treated with 1 μM STS for 10 h and subjected to the caspase 2 (open bar) or caspase 6 (hatched bar) activation assay. The mean $\pm$ S.D. of three experiments is presented. (**d**) Cells were treated with 1 μM STS for 5 h for the cytochrome *c* release assay or 10 h for other experiments. The cell lysates, or cytosol fraction for the cytochrome *c* release assay, were analyzed by immunoblotting with the indicated antibody. (**e**) The indicated cells were treated with 0.5 μM STS for 12 h and apoptosis was assessed. (**f**) The indicated cells were treated with 1 μM STS for 12 h and apoptosis was assessed

(*c-abl* + *arg*) RNAi cells are more prone to apoptosis, tumor growth was significantly repressed (Figures 7b, d). Tumor growth could be slightly rescued by the expression of wild-type Gal3 but not Gal3(Y79FY118F) (Figures 7c, d).

Discussion

Gal3 has previously been associated with several apoptotic mechanisms.[3,30,31] The phosphorylation of Gal3 at Ser6 and Ser12 by casein kinase has been extensively investi-
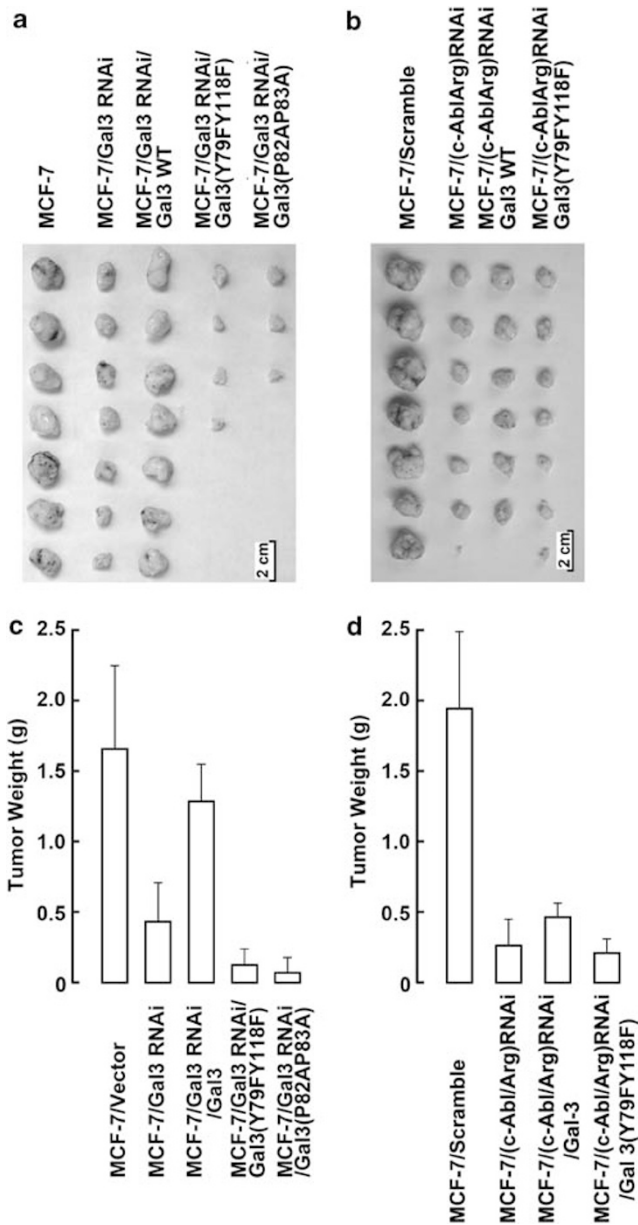
Figure 7 The c-Abl/Arg-mediated phosphorylation of Gal3 regulates tumorigenesis. (**a–d**) Female athymic nude mice (BALB/C nu/nu, 18–20 g) were subcutaneously inoculated at a single site with 5×106 cells as indicated. Tumors were surgically excised 21 days after inoculation (panels a, b) and weighed (panels **c**, **d**)

functions. Gal3 expression is downregulated in cells deficient in c-Abl or Arg, particularly in cells deficient in both tyrosine kinases. Both Gal3:Abl association and Gal3 tyrosine phosphorylation were significantly inhibited by high-level H_2O_2. CMA of Gal3 may have occurred in response to high-level oxidative stress conditions or high-dosage IR treatment.

The effect of STI571 on Gal3 expression was nowhere near the effect of Abl/Arg depletion, which suggests that, compared with the kinase activity, the presence of the Abl/Arg protein is more important in maintaining the intracellular levels of Gal3. The c-Abl/Arg-mediated phosphorylation of Gal3 may increase the Gal3 level by potentiating the c-Abl:Gal3 complex formation (Figures 1d–f). Cells deficient in either c-Abl or Arg were not as sensitive to the stimuli because the Gal3 levels were retained in the presence of either kinase. On the contrary, depleting c-Abl may result in attenuated apoptosis induced by DNA damage or oxidative stress through other apoptotic pathways.[6,10,16,21,34,35] Our results suggest that, depending on the cellular context, c-Abl/Arg can be proapoptotic or antiapoptotic through different pathways, and c-Abl/Arg-regulated lysosomal degradation of antiapoptotic Gal3 may provide one of the important arms in c-Abl/Arg-dependent antiapoptotic pathways.

There are 14 members in the Galectins family that share remarkable sequence similarities in the carbohydrate-recognition domain. Galectins are capable of controlling cell death in eukaryotic development, immune system homeostasis, and tumorigenesis.[36,37] Gal3 is the only member in the Galectin family that acts as an anti-apoptotic molecule. It differs from other Galectins in that it contains two galactose-binding domains and, importantly, an NWGR motif that is highly conserved among members of the Bcl2 family. This motif may be essential for its antiapoptotic properties by preventing mitochondrial damage, cytochrome c release, and caspase activation in response to various apoptotic stimuli.[4] Gal1, on the other hand, induces apoptosis of activated human T cells and human leukemia cells dependent on the expression of CD45.[38] Downregulation of Gal1 induces lysosomal membrane permeabilization in B16F10 mouse melanoma cells, possibly by the repression of HSP70 transcription controlled by certain Gal1-targeted NFAT.[39,40] In this study, c-Abl/Arg inhibitors induced lysosomal accumulation degradation of Gal3, with more HSP70 accumulated in the lysosomes (Figures 4 and 5a). The structural difference between Gal3 and other Galectins may confer differential consequences.

Using xenograft models, we confirmed that c-Abl/Arg is important in Gal3-mediated tumor generation. The observation that tumor size is even further attenuated by the expression of Gal3(Y79FY118F) and Gal3(P82AP83A) may be indicative of a dominant-negative effect of the mutant protein. The expression of an N-terminal truncated Gal3 has previously been shown to have a dominant-negative effect.[41] We also found that tumor growth could not be rescued by either wild-type or mutated Gal3 in c-Abl/Arg knockdown tumor cells, suggesting that the oncogenicity of Gal3 is dependent on the activity of c-Abl or Arg.

Gal3 is a tumorigenic protein that is overexpressed in many tumors. c-Abl inhibitor-induced lysosomal degradation of Gal3 may provide a new approach for tumor therapy.

gated.[32,33] In this study, we have shown that Gal3 is associated with and phosphorylated by c-Abl/Arg tyrosine kinases and the function of Gal3 in apoptosis, which is directly relevant to its association with the kinases.

Many of the other proteins that interact with and are phosphorylated by c-Abl are known to do so under stress-related conditions.[13] In contrast, the association of Gal3 with c-Abl and Arg is readily displayed, and strong tyrosine phosphorylation was also observed under steady-state conditions. These findings are relevant to physiological

Materials and Methods

Cell culture and transfections. 293T, MCF-7, HeLa, H1299, and MEFs derived from wild-type, c-abl$^{-/-}$, and c-abl$^{-/-}$arg$^{-/-}$ littermates[16] were grown in Dulbecco's modified Eagle's medium (DMEM; Invitrogen, Carlsbad, CA, USA) supplemented with 10% heat-inactivated fetal bovine serum (Hyclone, Mountain View, CA, USA), 2 mM L-glutamine, 100 Units/ml penicillin, and 100 μg/ml streptomycin. Transient transfections were performed with Lipofectamine 2000 (Invitrogen). Cells were also treated with STS, CDDP, 3MA, Concanamycin, lactocystin, PepA (all from Sigma, Louis, MO, USA) or STI571 (Novartis, ShangHai, China) as indicated.

Vectors and epitope tagging of proteins. Flag- or Myc-tagged c-Abl, Arg, Gal3, and their mutants were expressed by cloning the genes into the pcDNA3-based Flag vector (Invitrogen) or pCMV-Myc (Clontech, Otsu, shiga, Japan). GST fusion proteins were generated by expression in pGEX4T-2-based vectors (Amersham Biosciences Biotech Inc., Piscataway, NJ, USA) in *Escherichia coli* BL21 (DE3). Site mutations in c-Abl and Gal3 genes were achieved by overlapping PCR.

Immunoprecipitation and immunoblot analysis. Cell lysates were prepared in lysis buffer (50 mM Tris-HCl (pH 7.5), 1 mM phenylmethylsulfonyl fluoride, 1 mM dithiothreitol, 10 mM sodium fluoride, 10 μg/ml aprotinin, 10 μg/ml leupeptin, and 10 μg/ml PepA) containing 1% Nonidet P-40. Soluble proteins were subjected to immunoprecipitation with anti-Flag (M2, Sigma), anti-Myc (9E10, Santa Cruz, Santa Cruz, CA, USA), anti-Gal3 (B2 mouse monoclonal antibody, Santa Cruz), or anti-c-Abl (K-12 rabbit polyclonal antibody, Santa Cruz). Normal rabbit IgG or normal mouse IgG of the same subclass (Santa Cruz) was used as the control. In addition, an aliquot of the total lysate (5%, v/v) was included as a control. Immunoblot analysis was performed with horseradish peroxidase (HRP)-conjugated anti-Myc (9E10, Santa Cruz), HRP-conjugated anti-Flag (M2, Sigma), anti-β-actin (Sigma), anti-α-tubulin (Sigma), HRP-conjugated anti-P-Tyr (4G10, Upstate Biotechnology Inc., Temecula, CA, USA), anti-HSC70 (H-300, Santa Cruz), anti-Gal3 (H160, rabbit polyclonal antibody, Santa Cruz), anti-c-Abl (24–11, mouse monoclonal antibody, Santa Cruz), or anti-LamP2 (H4B4, Santa Cruz) antibody. The antigen-antibody complexes were visualized with chemiluminescence (Perkin-Elmer Life Sciences Inc., Waltham, MA, USA). TRUE Western marker (Vigorous) was used as a molecular weight standard.

To confirm that protein interaction occurred in the cells, 5×10^6 cells were treated with 1 ml 1.0% w/v cross-linking paraformaldehyde (PFA) in PBS for 30 min, and the reaction was stopped by adding glycine at a final concentration of 125 mM. Cell lysates were prepared in lysis buffer containing 25 mM lactose,[31] as described above, and the supernatants were subjected to immunoprecipitation.[42]

Protein-binding assays. In GST pull-down experiments, cell lysates were incubated for 2 h at 4°C with 2 μg purified GST or GST fusion proteins bound to glutathione beads (GE Healthcare, Little Chalfont, Buckinghamshire, UK). The adsorbates were washed with lysis buffer and then subjected to SDS-PAGE and immunoblot analysis. An aliquot of the total lysate (5%, v/v) was included as a loading control.

In direct binding assays, immunoprecipitates were separated by SDS-PAGE and then blotted onto nitrocellulose membranes. The membranes were subsequently incubated with purified GST fusion proteins for 2 h at room temperature. The GST fusion proteins binding to the nitrocellulose were probed with anti-GST antibody.

Kinase assays. Purified recombinant Gal3 (0.5 μg; CytoLab Ltd, Rocky Hill, NJ, USA) was incubated with recombinant c-Abl and Arg (0.02 μg; Upstate Biotechnology Inc.) in kinase buffer (20 mM HEPES (pH 7.5), 75 mM KCl, 10 mM MgCl$_2$, and 10 mM MnCl$_2$) containing 2.5 μCi of [γ-^{32}P] ATP for 30 min at 37°C. The reaction products were analyzed by SDS-PAGE and autoradiography.

Pulse-chase assays. Cells were transfected with Flag-Gal3 or Gal3 mutants for 18 h, and then incubated with methionine-free DMEM (Invitrogen) containing 10 μCi/ml [^{35}S]methionine (Amersham Biosciences Biotech Inc.) for 90 min. The cells were then washed and cultured in complete DMEM and harvested at the indicated time points. Anti-Flag immunoprecipitates were subjected to SDS-PAGE and autoradiography. The bands were excised and subjected to liquid scintillation counting for quantitation.

LC/MS/MS. After the gel was stained with Coomassie Blue, the protein band was excised from the gel and minced into pieces. Dried gel pieces were incubated with 10 μl porcine elastase (Roche, Indianapolis, IN, USA) for 16 h at 37°C. The peptide mixtures were extracted by acetonitrile/water (1:1, v/v) with 0.1% formic acid solution. Nano-LC-MS/MS analysis was carried out on an LC-Packing System (Dionex/LC Packings, Sunnyvale, CA, USA) coupled with a hybrid linear ion trap-7T Fourier transform ion cyclotron resonance mass spectrometer (LTQFTMS, Thermo Electron, Waltham, MA, USA). One full MS scan (400–2000 m/z, 10^5 resolution in ICR cell and automatic gain control (AGC) of 5×10^5) was followed by 10 data-dependent MS/MS spectra in the linear ion trap from the 10 most abundant ions and with dynamic exclusion for 30 s. Singly charged ions were rejected. Data were analyzed by searching against the database using a local Mascot search engine (v2.1, Matrix Science, Boston, MA, USA) filtered by a mascot score ≥25. The filtered phosphopeptides were validated by manually interpreting the MS/MS spectra.

Immunofluorescence and confocal microscopy. The immuno-fluorescent staining of cells was performed as described previously.[43] Briefly, the cells were fixed with 4% PFA for 15 min, permeabilized with 0.5% Triton X-100 for 10 min, and blocked with 1% goat serum albumin in PBS for 30 min. Anti-Gal3, anti-Lamp2, anti-HSC70, or anti-LC3 (Abgent, San Diego, CA, USA) antibody was added and incubated for 1 h at room temperature. FITC- or TRITC-conjugated goat anti-mouse or anti-rabbit immunoglobulin (Jackson ImmunoResearch Inc., West Grove, Pennsylvania, USA) was added and incubated for another 1 h. Confocal microscopy was performed using a Bio-Rad Radiance 2100 microscope (Bio-Rad, Hercules, CA, USA) equipped with a × 150 objective lens. The percentage of Gal3 accumulated in lysosomes or with HSP70 was assessed by densitometry (Tanon, Ver2.0, Shang hai, China).

Preparation of lysosomes. Lysosomes were prepared from cells by Percoll/metrizamide gradient centrifugation as described previously.[44] Briefly, 2×10^7 cells were incubated with hypotonic buffer and homogenized with a B-type Dounce homogenizer. The homogenate was centrifuged at 1300 g for 5 min, and the supernatant was subjected to centrifugation using hybrid Percoll-metrizamide sequential density gradients at 50 500 g for 15 min at 4°C, and then the interfaces were collected.

Apoptosis assay. The DNA content of the cell was assessed by staining ethanol-fixed and citrate buffer-treated cells with propidium iodide and monitoring by FACScan (Becton-Dickinson, Franklin Lakes, NJ, USA). The number of cells with sub-G1 DNA, an indicator of apoptotic cells, was determined with a MODFIT LT program. The percentage of apoptotic cells was expressed as the mean ± S.D. of three experiments.

Cytochrome c release assay. Cell pellets were resuspended in 1 ml ice-cold buffer A (250 mM sucrose, 20 mM HEPES (pH 7.4), 10 mM KCl, 1.5 mM MgCl$_2$, 1 mM EDTA, 1 mM EGTA, 1 mM dithiothreitol, 170 μg/ml phenylmethylsulfonyl fluoride, 16 μg/ml aprotinin, and 4 μg/ml leupeptin) and incubated for 10 min on ice. Cells were lysed by a Wheaton overhead stirrer (Wheaton, Wheaton, IL, USA). Unlysed cells and nuclei were pelleted at 120 g for 10 min at 4°C. The supernatant was centrifuged at 10 000 g at 4°C for 25 min, and then at 100 000 g for 1 h at the same temperature. Equal amounts of the supernatant were subjected to western blotting with anti-cytochrome c.

Caspase activation assay. A total of 3×10^6 cells were treated with STS for 10 h, resuspended in 50 μl of cell lysis buffer from the Caspase Fluorometric Assay Kit (Biovision, Mountain View, CA, USA), and then incubated for 10 min on ice. A 100 μl aliquot of the cell lysate was incubated with caspase substrates (caspase 2, VDVAD-AFC; caspase 6, VEID-AFC; caspase 12, ATAD-AFC) for 2 h. Relative fluorescence was assayed at an excitation wavelength of 400 nm and an emission wavelength of 505 nm using a fluorescence spectrometer (Thermo Fluoroskan, Waltham, MA, USA). Relative fluorescence intensity was calculated as the mean ± S.D. of three experiments.

***In vivo* tumorigenicity assay.** Female athymic nude mice (Balb/c nu/nu, 18–20 g) were randomly divided into groups and subcutaneously inoculated at a single site with 5×10^6 tumor cells. Tumor diameter was measured weekly using calipers until 21 days when the tumor weight was also determined after dissection.

RNA interference. The siRNA sequences targeting mRNAs were as follows Gal3, GCTCACTTGTTGCAGTACA; c-Abl and Arg (co-RNAi), GGGAAATTGCT ACCTATGG, which is 100% homologous between c-Abl and Arg; and the nonsilencing scramble sequence, GTGACATAGCAGGAACTAC. These sequences were cloned into the pSUPER-retro-neo plasmid (OligoEngine Inc., Seattle, WA, USA) or psiSTRIKETM-Hygromycin Vector (Promega, Madison, WI, USA). The rescue of Gal3 or its mutants was achieved by the stable transfection of the expression vector in which three nucleotides in the Gal3 targeting sequences were mutated without any amino-acid changes. Stable cell lines were obtained by treating the cells with 800 μg/ml G418, 50 μg/ml hygromycin B, and/or 2 μg/ml puromycin. Individual clones were picked and identified by RT-PCR and western blot for the relevant protein.

Conflict of interest

The authors declare no conflict of interest.

1. Nangia-Makker P, Honjo Y, Sarvis R, Akahani S, Hogan V, Pienta KJ *et al*. Galectin-3 induces endothelial cell morphogenesis and angiogenesis. *Am J Pathol* 2000; **156**: 899–909.
2. Liu FT, Rabinovich GA. Galectins as modulators of tumour progression. *Nat Rev Cancer* 2005; **5**: 29–41.
3. Akahani S, Nangia-Makker P, Inohara H, Kim HR, Raz A. Galectin-3: a novel antiapoptotic molecule with a functional BH1 (NWGR) domain of Bcl-2 family. *Cancer Res* 1997; **57**: 5272–5276.
4. Yu F, Finley Jr RL, Raz A, Kim HR. Galectin-3 translocates to the perinuclear membranes and inhibits cytochrome *c* release from the mitochondria. A role for synexin in galectin-3 translocation. *J Biol Chem* 2002; **277**: 15819–15827.
5. Van Etten RA. Cycling, stressed-out and nervous: cellular functions of c-Abl. *Trends Cell Biol* 1999; **9**: 179–186.
6. Pendergast AM. The Abl family kinases: mechanisms of regulation and signaling. *Adv Cancer Res* 2002; **85**: 51–100.
7. Wang JY. Regulation of cell death by the Abl tyrosine kinase. *Oncogene* 2000; **19**: 5643–5650.
8. Pendergast AM. Stress and death: breaking up the c-Abl/14-3-3 complex in apoptosis. *Nat Cell Biol* 2005; **7**: 213–214.
9. Goga A, Liu X, Hambuch TM, Senechal K, Major E, Berk AJ *et al*. p53 dependent growth suppression by the c-Abl nuclear tyrosine kinase. *Oncogene* 1995; **11**: 791–799.
10. Yuan ZM, Huang Y, Fan MM, Sawyers C, Kharbanda S, Kufe D. Genotoxic drugs induce interaction of the c-Abl tyrosine kinase and the tumor suppressor protein p53. *J Biol Chem* 1996; **271**: 26457–26460.
11. Yuan ZM, Shioya H, Ishiko T, Sun X, Gu J, Huang YY *et al*. p73 is regulated by tyrosine kinase c-Abl in the apoptotic response to DNA damage. *Nature* 1999; **399**: 814–817.
12. Agami R, Blandino G, Oren M, Shaul Y. Interaction of c-Abl and p73alpha and their collaboration to induce apoptosis. *Nature* 1999; **399**: 809–813.
13. Sun X, Majumder P, Shioya H, Wu F, Kumar S, Weichselbaum R *et al*. Activation of the cytoplasmic c-Abl tyrosine kinase by reactive oxygen species. *J Biol Chem* 2000; **275**: 17237–17240.
14. Cao C, Leng Y, Kufe D. Catalase activity is regulated by c-Abl and Arg in the oxidative stress response. *J Biol Chem* 2003; **278**: 29667–29675.
15. Dorsch M, Goff SP. Increased sensitivity to apoptotic stimuli in c-abl-deficient progenitor B-cell lines. *Proc Natl Acad Sci USA* 1996; **93**: 13131–13136.
16. Koleske AJ, Gifford AM, Scott ML, Nee M, Bronson RT, Miczek KA *et al*. Essential roles for the Abl and Arg tyrosine kinases in neurulation. *Neuron* 1998; **21**: 1259–1272.
17. Amarante-Mendes GP, Naekyung Kim C, Liu L, Huang Y, Perkins CL, Green DR *et al*. Bcr-Abl exerts its antiapoptotic effect against diverse apoptotic stimuli through blockage of mitochondrial release of cytochrome C and activation of caspase-3. *Blood* 1998; **91**: 1700–1705.
18. Van Etten RA, Jackson P, Baltimore D. The mouse type IV c-abl gene product is a nuclear protein, and activation of transforming ability is associated with cytoplasmic localization. *Cell* 1989; **58**: 669–678.
19. McGahon A, Bissonnette R, Schmitt M, Cotter KM, Green DR, Cotter TG. BCR-ABL maintains resistance of chronic myelogenous leukemia cells to apoptotic cell death. *Blood* 1994; **83**: 1179–1187.
20. Barila D, Superti-Furga G. An intramolecular SH3-domain interaction regulates c-Abl activity. *Nat Genet* 1998; **18**: 280–282.
21. Deng X, Hofmann ER, Villanueva A, Hobert O, Capodieci P, Veach DR *et al*. Caenorhabditis elegans ABL-1 antagonizes p53-mediated germline apoptosis after ionizing irradiation. *Nat Genet* 2004; **36**: 906–912.
22. Gong JG, Costanzo A, Yang HQ, Melino G, Kaelin WG, Jr., Levrero M, Wang JY. The tyrosine kinase c-Abl regulates p73 in apoptotic response to cisplatin-induced DNA damage. *Nature* 1999; **399**: 806–809.
23. Vigneri P, Wang JY. Induction of apoptosis in chronic myelogenous leukemia cells through nuclear entrapment of BCR-ABL tyrosine kinase. *Nat Med* 2001; **7**: 228–234.
24. Barila D, Rufini A, Condo I, Ventura N, Dorey K, Superti-Furga G *et al*. Caspase-dependent cleavage of c-Abl contributes to apoptosis. *Mol Cell Biol* 2003; **23**: 2790–2799.
25. Baskaran R, Wood LD, Whitaker LL, Canman CE, Morgan SE, Xu Y *et al*. Ataxia telangiectasia mutant protein activates c-Abl tyrosine kinase in response to ionizing radiation. *Nature* 1997; **387**: 516–519.
26. Majeski AE, Dice JF. Mechanisms of chaperone-mediated autophagy. *Int J Biochem Cell Biol* 2004; **36**: 2435–2444.
27. Agarraberes FA, Terlecky SR, Dice JF. An intralysosomal hsp70 is required for a selective pathway of lysosomal protein degradation. *J Cell Biol* 1997; **137**: 825–834.
28. Mooney LM, Al-Sakkaf KA, Brown BL, Dobson PR. Apoptotic mechanisms in T47D and MCF-7 human breast cancer cells. *Br J Cancer* 2002; **87**: 909–917.
29. Nakahara S, Oka N, Raz A. On the role of galectin-3 in cancer apoptosis. *Apoptosis* 2005; **10**: 267–275.
30. Fukumori T, Takenaka Y, Oka N, Yoshii T, Hogan V, Inohara H *et al*. Endogenous galectin-3 determines the routing of CD95 apoptotic signaling pathways. *Cancer Res* 2004; **64**: 3376–3379.
31. Yang RY, Hsu DK, Liu FT. Expression of galectin-3 modulates T-cell growth and apoptosis. *Proc Natl Acad Sci USA* 1996; **93**: 6737–6742.
32. Huflejt ME, Turck CW, Lindstedt R, Barondes SH, Leffler H. L-29, a soluble lactose-binding lectin, is phosphorylated on serine 6 and serine 12 *in vivo* and by casein kinase I. *J Biol Chem* 1993; **268**: 26712–26718.
33. Yoshii T, Fukumori T, Honjo Y, Inohara H, Kim HR, Raz A. Galectin-3 phosphorylation is required for its anti-apoptotic function and cell cycle arrest. *J Biol Chem* 2002; **277**: 6852–6857.
34. Raina D, Ahmad R, Kumar S, Ren J, Yoshida K, Kharbanda S *et al*. MUC1 oncoprotein blocks nuclear targeting of c-Abl in the apoptotic response to DNA damage. *EMBO J* 2006; **25**: 3774–3783.
35. Huang Y, Yuan ZM, Ishiko T, Nakada S, Utsugisawa T, Kato T *et al*. Pro-apoptotic effect of the c-Abl tyrosine kinase in the cellular response to 1-beta-D-arabinofuranosylcytosine. *Oncogene* 1997; **15**: 1947–1952.
36. Hernandez JD, Baum LG. Ah, sweet mystery of death! Galectins and control of cell fate. *Glycobiology* 2002; **12**: 127R–136R.
37. Rabinovich GA, Toscano MA. Turning 'sweet' on immunity: galectin-glycan interactions in immune tolerance and inflammation. *Nat Rev Immunol* 2009; **9**: 338–352.
38. Perillo NL, Pace KE, Seilhamer JJ, Baum LG. Apoptosis of T cells mediated by galectin-1. *Nature* 1995; **378**: 736–739.
39. Mathieu V, Le Mercier M, De Neve N, Sauvage S, Gras T, Roland I *et al*. Galectin-1 knockdown increases sensitivity to temozolomide in a B16F10 mouse metastatic melanoma model. *J Invest Dermatol* 2007; **127**: 2399–2410.
40. Le Mercier M, Lefranc F, Mijatovic T, Debeir O, Haibe-Kains B, Bontempi G *et al*. Evidence of galectin-1 involvement in glioma chemoresistance. *Toxicol Appl Pharmacol* 2008; **229**: 172–183.
41. Hoyer KK, Pang M, Gui D, Shintaku IP, Kuwabara I, Liu FT *et al*. An anti-apoptotic role for galectin-3 in diffuse large B-cell lymphomas. *Am J Pathol* 2004; **164**: 893–902.
42. Vasilescu J, Guo X, Kast J. Identification of protein-protein interactions using *in vivo* cross-linking and mass spectrometry. *Proteomics* 2004; **4**: 3845–3854.
43. Tsay YG, Lin NY, Voss PG, Patterson RJ, Wang JL. Export of galectin-3 from nuclei of digitonin-permeabilized mouse 3T3 fibroblasts. *Exp Cell Res* 1999; **252**: 250–261.
44. Storrie B, Madden EA. Isolation of subcellular organelles. *Methods Enzymol* 1990; **182**: 203–225.

Supplementary Information accompanies the paper on Cell Death and Differentiation website (http://www.nature.com/cdd)